

Simulation of Counter-current Spontaneous Imbibition in a Simple Porous Medium Using Lattice-Boltzmann

Rasoul Arabjamaloei and Douglas Ruth

University of Manitoba

This paper was prepared for presentation at the International Symposium of the Society of Core Analysts held in Avignon, France, 8-11 September, 2014

ABSTRACT

The lattice Boltzmann method (LBM) has been increasingly implemented for complicated fluid flow and transport phenomena. In this paper the LBM method is utilized to simulate the experimental results of counter current spontaneous imbibition. The single component multiphase Shan-Chen model was used to model the antiparticle forces. It was observed in the results that the developed model, although it simulated the shape of the front, it did not lead to bubble snap-off caused by capillary instability and the pressure at the dead end of the imbibition channel does not match with experimental results.

1. INTRODUCTION

The simplicity of application of the LBM for complicated geometries is one of the main reasons for the popularity of this method. Unlike the computational fluid dynamic (CFD) method, LBM is a mesoscopic approach which has some benefits of microscopic modeling with affordable computational expenses [4]. At the microscopic scale, fluid is formed by particles moving in all directions and constantly colliding and bouncing back from boundaries. Modeling the exact behavior of all the particles is practically impossible due to the huge number of particles and computational processor's limitations. At the mesoscale however, instead of considering the individual particles, the LBM evolves particle distribution functions with a set of fixed velocities at discrete locations in space [5]. It has been shown that the macroscopic fluid properties (density and velocities) obtained by averaging the particle distribution satisfy the Navier–Stokes equations [1, 6].

In classic fluid mechanics the behavior of a fluid is modeled by governing equations which are derived by applying conservation of mass, energy and momentum on an infinitesimal volume. These equations have the form of partial differential equations and might be solved analytically or numerically at discrete locations of space and time using initial and boundary conditions. Considering the advances in current CFD, one might ask what is the necessity of using a particle based method like lattice Boltzmann? Lattice Boltzmann is an alternative method for CFD with the benefit of lower computational expenses, simplicity of application for complex transport media, simple parallelization,

and automatic interface tracking. LBM has been successfully used in a variety of fluid flow in porous media [2] and multiphase flow problems [3, 11, 10, 12].

2. METHODOLOGY

2.1 Model Geometry

Unsal *et al.* performed co-current and counter-current experiments using a glass and rod model [15]. In their model two separate or three interconnected irregular shaped capillary channels were the transport medium. Three types of fluids (Liquid paraffin, Isooctane and air) were used for two-phase displacement processes. The experimental set-up was such that the interface could be observed and the pressure at several points could be recorded. Figure 1 shows the rod and glass structure. In the present study, multiphase LBM model is used in an attempt to reproduce the results reported by Unsal *et al.* [15].

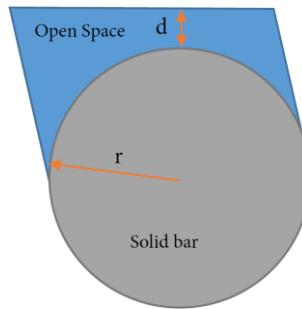


Figure 1: The Glass and rod model forming a flow pass for spontaneous imbibition [15].

2.2 Lattice Boltzmann for Fluid Dynamics

2.2.1 Single Phase, Single Component Fluid

The general discretized form of the lattice Boltzmann equation derived by using the BGK approximation for a single component can be written as [17]:

$$f_i(x + c_i \Delta t, t + \Delta t) = f_i(x, t) - \frac{f_i(x, t) - f_i^{eq}(x, t)}{\tau} \quad (1)$$

Here $f_i(x, t)$ is the distribution function along the lattice direction i at location x and time t , c_i 's are the velocity unit vectors, τ is the collision relaxation time and $f_i^{eq}(x, t)$ is the equilibrium distribution function. This equation is applied in lattice space where the velocity directions are finite and predefined. Based on the number of space dimensions and the number of velocity directions, the common lattice spaces are D1Q2, D1Q3, D2Q9, D3Q15 and D3Q19, where D# is the number of space dimensions and Q# is the number of velocity directions. In the present study D3Q15 (three dimensional with 15 velocity directions) is used. Figure 2 shows this lattice mode where number 1 is the central node.

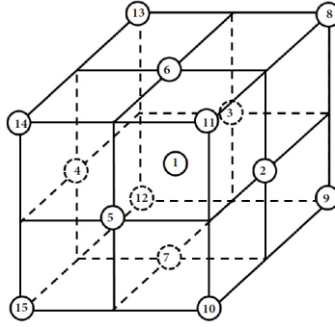


Figure 2: A typical D3Q15 lattice. The velocity directions are from the central node (number 1) to the other 14 nodes.

In D3Q15 lattice space the velocity unit vectors are as follows:

$$\mathbf{c} = c \begin{bmatrix} 0 & 1 & 0 & -1 & 0 & 0 & 0 & 1 & 1 & 1 & 1 & -1 & -1 & -1 & -1 \\ 0 & 0 & 1 & 0 & -1 & 0 & 0 & 1 & 1 & -1 & -1 & 1 & 1 & -1 & -1 \\ 0 & 0 & 0 & 0 & 0 & 1 & -1 & 1 & -1 & -1 & 1 & -1 & 1 & 1 & -1 \end{bmatrix}$$

The equilibrium distribution function obtained by the BGK approximation is:

$$f_i^{eq}(x, t) = w_i \rho \left[1 + 3 \frac{c_i \cdot u^{eq}}{c^2} + \frac{9}{2} \frac{(c_i \cdot u^{eq})^2}{c^4} - \frac{3}{2} \frac{(u^{eq})^2}{c^2} \right] \quad (2)$$

In this equation ρ is the lattice density, c is the lattice speed and w_i are the weights associated with different lattice directions, given below:

$$w_i = \begin{cases} \frac{16}{72} & i = 0 \\ \frac{8}{72} & i = 1, 2, 3, 4, 5, 6, 7, 8 \\ \frac{1}{72} & i = 9, 10, 11, 12, 13, 14, 15 \end{cases} \quad (3)$$

The macroscopic hydrodynamic properties are obtained from the distribution functions as:

$$\rho(x, t) = \sum_{i=0}^{15} f_i(x, t) \quad (4)$$

$$u(x, t) = \frac{1}{\rho} \sum_{i=0}^{15} c_i f_i(x, t) \quad (5)$$

Here $\rho(x, t)$ and $u(x, t)$ are the lattice density and velocity vector at location x and time t .

The kinematic viscosity is defined as:

$$\vartheta = \frac{1}{3} c^2 \left(\tau - \frac{1}{2} \right) \quad (6)$$

2.2.2 Multiphase, Multicomponent Flow

The LBM can be applied for systems consisting of more than one phase and one component. There are three major methods for multicomponent multiphase problems including the Shan-Chen pseudo potential model [11, 13], the free energy model [14], and the colour gradient model. In this research we used the Shan-Chen model. For the multiphase/multicomponent systems the parameter u^{eq} in equation 2 is modified as:

$$u_k^{eq} = u' + \tau_k F_k \quad (7)$$

Here u' is the total velocity given by

$$u' = \left(\sum_{k=1}^s \frac{\rho_k u_k}{\tau_k} \right) / \left(\sum_{k=1}^s \frac{\rho_k}{\tau_k} \right) \quad (8)$$

Further k is the index of fluids, F_k is the total interaction force which is the sum of three distinct forces:

$$F_k = F_{1k} + F_{2k} + F_{3k} \quad (9)$$

Here F_{1k} is the fluid-fluid interaction, F_{2k} is the fluid-solid interaction and F_{3k} is the external force (such as gravity) [9].

The fluid-fluid particle interaction force at location x is defined as [7]:

$$F_{1k}(x) = -\varphi_k(x) \sum_{x'} \sum_{\bar{k}=1}^s G_{k\bar{k}}(x, x') \varphi_{\bar{k}}(x') (x - x') \quad (10)$$

In this equation $G_{k\bar{k}}$ is the strength of fluid-fluid particles interaction force, φ is the effective density and the index s shows the total number of fluid components. The above equation in lattice form for D3Q15 is:

$$F_{1k}(x) = -G_{k\bar{k}} \varphi_k(x) \sum_{i=0}^{15} w_i(|e_i|) \varphi_{\bar{k}}(x + e_i) e_i \quad (11)$$

Different forms of effective density have been used such as

$$\varphi(\rho) = \rho_0 \left[1 - \exp \left(-\frac{\rho}{\rho_0} \right) \right] \quad (12)$$

or

$$\varphi(\rho) = \varphi_0 \exp \left(-\frac{\rho_0}{\rho} \right) \quad (13)$$

Here φ_0 and ρ_0 are constants which are commonly set to 4 and 0 respectively. When the density ratio of the two components is high or when modeling multiphase systems, different equations of state must be combined with the above mentioned effective mass equations. This requirement will be explained further in the following sections.

The fluid-solid particle interaction force in lattice form is defined as:

$$F_{2k}(x) = -G_{ad,k} \varphi_k(x) \sum_{i=0}^{15} w_i(|e_i|) S(x + e_i) e_i \quad (13)$$

Here $S(x+e_i)$ is an indicator which is 1 for the solid and 0 for the fluid in the neighbour node and $G_{ad,k}$ is the interaction strength of the solid surface and fluid component k .

The force associated with body forces (such as gravity) is defined as:

$$F_{3k}(x) = -\rho_k(x)g \quad (13)$$

where g is the body force per unit mass.

2.2.3 Equations of state

Equations of state (EOS) represent the relationship between the fluid pressure, temperature and density. If the particle interaction force is given by equation 10, the EOS of the system for D3Q15 lattice model becomes [16],

$$P = \frac{\rho}{3} + 5g(\varphi(\rho))^2 \quad (14)$$

The original Shan-Chen model works well in single phase and in multicomponent systems where the two components have the same density [16]. Yuana and Schaefer studied the possibility and the effect of using different equations of states in conjunction with the Shan-Chen model and reported that by using the Canahan-Starling (C-S) EOS high density ratios are achievable [16]. In this research we use the C-S EOS which is:

$$P = \rho RT \frac{1 + b\rho/4 + (b\rho/4)^2 - (b\rho/4)^3}{(1 - b\rho/4)^3} - a\rho^2 \quad (15)$$

Where

$$a = 0.4963R^2T_c^2/P_c \quad (16)$$

$$b = 0.18727RT_c/P_c \quad (17)$$

Here a , b and R are set to 1, 4 and 1 respectively. To achieve phase separation using the above EOS the proper value of T should be used. Figure 3 shows the pressure density curve for different ratios of temperature (T) to the critical temperature (T_c).

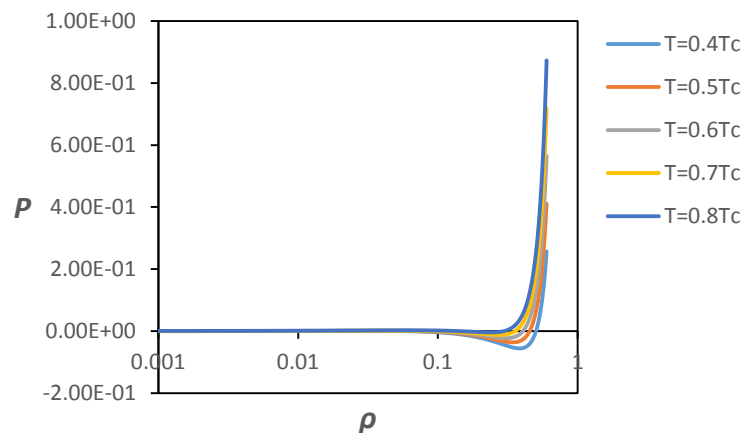


Figure 3: Pressure-density curves resulted by C-S equation of state.

If we zoom in on the density region of 0.001 to 0.1 we see that two different densities can coexist at the same pressure, a physical impossibility.

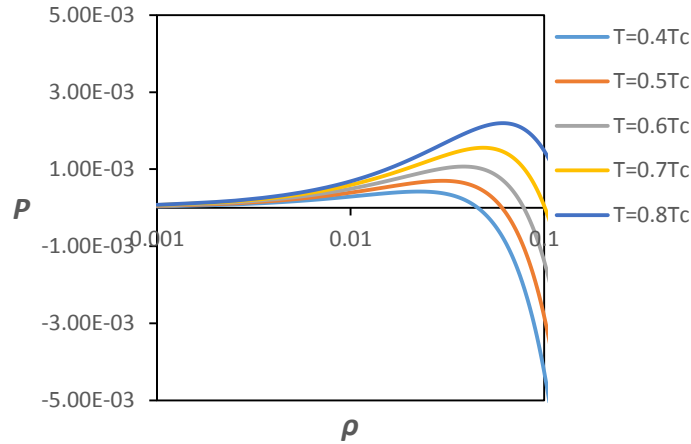


Figure 4: Pressure-density curves resulted by C-S equation of state for the density range of 0.001-0.1.

3. APPROACH WITH LBM

In this research, the single component multiphase (SCMP) Shan-Chen model was used to simulate air-water systems. The capillary rise phenomena has been studied using the SCMP model and the results have been shown to be satisfactory [8]. To develop the desired LB model we should go through some steps to test the features of the model. These steps are a phase separation test, contact angle measurement, capillary rise and gravity check, and a bubble snap off analysis.

3.1 Phase Separation

To investigate phase separation, a density distribution of 0.07 plus a random number in the range of -0.001 and 0.001 was set as the initial density for a mesh of 200×200 lattice nodes. The attraction strength was set to -30 and the temperature was set to $T=0.6T_c$. Figure 5 shows the phase separation stages.

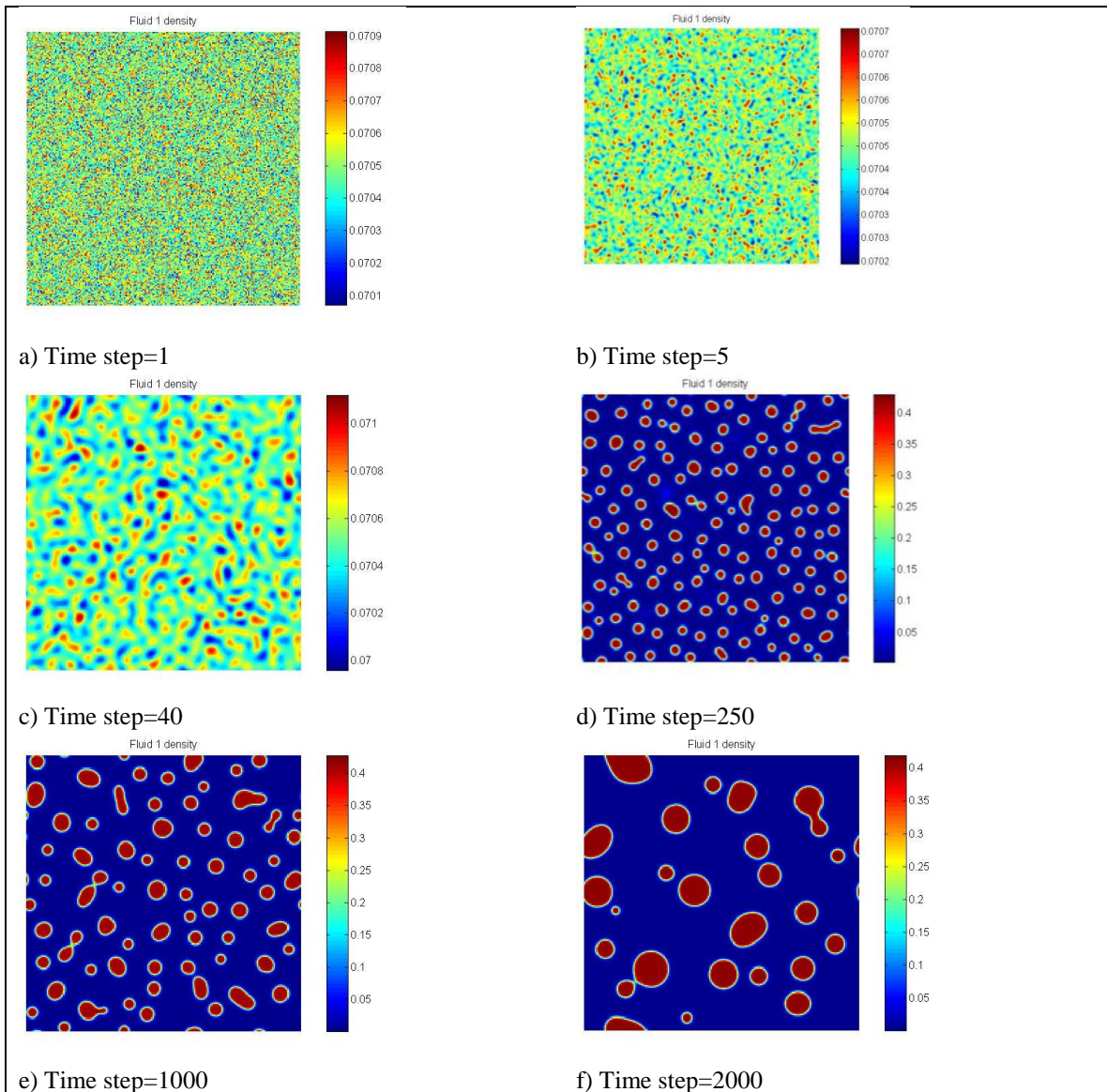


Figure 5: The process of phase separation from a uniform density distribution.

As can be seen in figure 5, phase separation occurs and two phases appear. Further, with an appropriate choice of initial density, two phases with the desired final densities can be produced. It is possible to reach a density (ratio?) of 1000 using C-S EOS [8]. However we observed that when the density ratio is higher than 50 in multiphase flow problems, it is difficult to prevent the solution from diverging. Therefore in the present paper we used a density ratio of 50 – in real air-water systems the density ratio is almost 800.

3.2 Contact Angle Measurement

The next step is to investigate the effect of solid-fluid interaction strength (G_{ad}) on droplet contact angle at the solid-fluid contact surface. A set of tests were ran to find this effect. Figure 6 illustrates different cases.

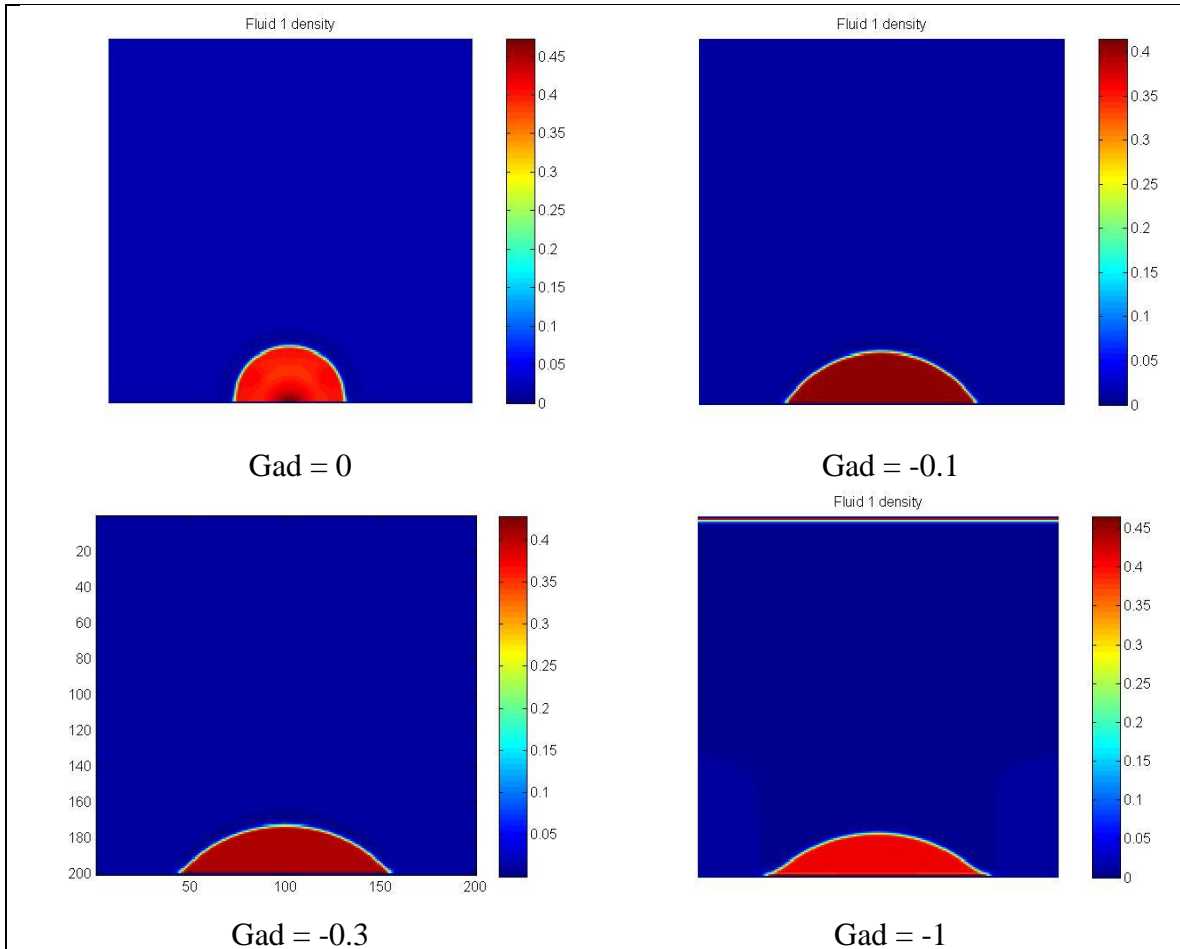


Figure 6: The effect of G_{ad} on contact angle.

Figure 6 demonstrates that the solid-fluid interaction strength can be set to adjust the problem for any desired contact angle.

3.3 Capillary Rise and gravity check

Capillary rise is the simplest form of spontaneous imbibition. Before advancing our model to complicated processes, we start by simulating the capillary rise phenomenon. The model consists of a liquid with density of 0.28 and a vapour with density of 0.05 in contact with a capillary channel in a two dimensional mesh. Figure 7 shows the schematic of the system.

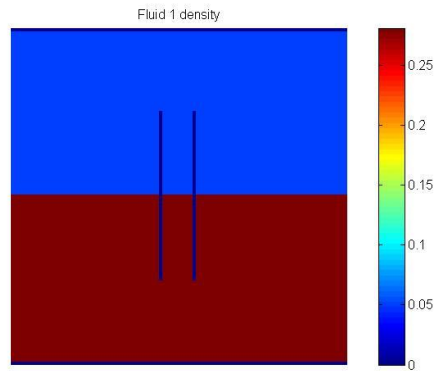


Figure 7: Initial condition for the capillary rise test

G_{ad} was set to -0.5 and the gravity coefficient was set to 0.00001 in lattice units. A mesh of size 200×200 was used and a capillary channel of size 20 in width was set at the center of the mesh. Initially, the bottom half of the system is filled with the liquid and the upper half with vapour. Bounce back boundary condition at the bottom and upper sides and periodic boundary condition at the right and left insures a realistic model. Figure 8 shows the progress of the liquid in the capillary. The general behaviour of the results is reasonable. In this model the outer layer of the wall is different than the inner wall such that the contact angle at the outer wall is 90° . The curvature formed at the area outside of the tube is due to particle attraction, small mesh size, gravity and tendency of the vapour to form a bubble.

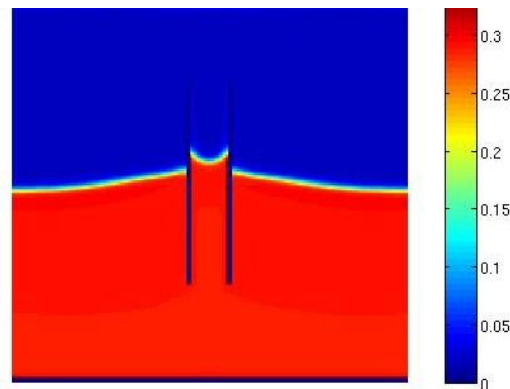


Figure 8: Capillary rise after 1000 time steps

3.4 Bubble snap off Analysis

Bubble snap off is a complicated phenomenon which can arise because of three reasons; capillary instability, buoyancy and shear force. Unsal *et al.* believed that the capillary instability is the cause of bubble snap off in their experiments [15]. To test if a two phase Shan-Chen model can simulate the snap off phenomenon in the absence of buoyancy and

shear force, a simple system was created. A 500×200 mesh (figure 9a) was formed where the fluid properties are the same as the capillary rise test. It was seen that in this model bubble snap off never occurs by the result of capillary instability. Since the Shan-Chen model is not verified to simulate this process it can't be concluded that in the Unsal *et al.* experiment the cause of the snap off was something other than capillary instability [15]. However, since we need the snap off to happen in our model, buoyancy force was inserted in the model by adding the gravity effect. As figure 9b-9f shows, by adding the gravity component, the bubbles stretches and pinches off.

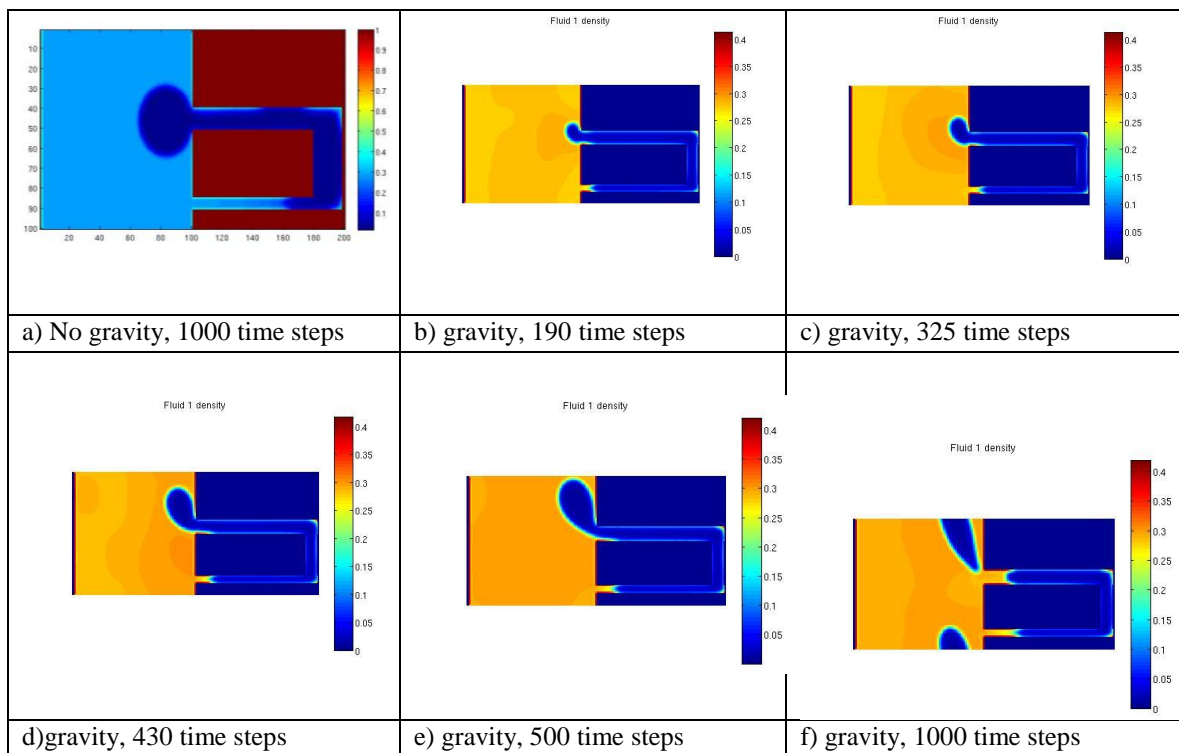


Figure 9: A simple countercurrent imbibition model with and without buoyancy effect

3.5 Unsal *et al.* Model

The developed model was modified to simulate the experiments by Unsal *et al.* [15]. A three dimensional mesh of size $60 \times 80 \times 2000$ was used to model a countercurrent displacement where there exists lateral connection between the channels. Vapour pressure at the farthest distance from the imbibition face and production rate of vapour were taken as results. Figure 10 shows the pressure at the closed end of the tubes.

4. DISCUSSION OF THE RESULTS AND CONCLUSIONS

As it is seen in figure 10 the pressure of the vapor phase goes up as the imbibition process proceeds. Unsal *et al.* reported that the pressure of the non-wetting phase drops while the bubble is forming and rises up suddenly when the bubble pinches off. However it is seen in our results that pressure just raises up by time. This is because the Shan-Chen method is not able to simulate the capillary instability phenomenon which is the cause of the bubble snap off. Figure 10 compares the obtained results in the present work and the Unsal *et al.* results.

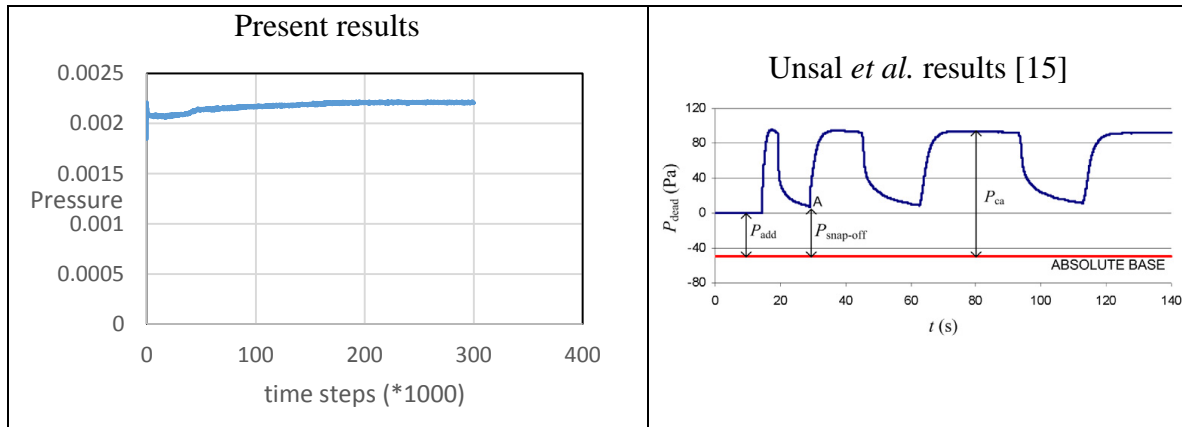


Figure 10: Pressure at the dead end of the tubes

ACKNOWLEDGEMENTS: Support for this work was provided by the National Science and Engineering Research Council of Canada.

REFERENCES

1. Frisch, U., Hasslacher, B., Pomeau, Y., "Lattice-Gas Automata for the Navier-Stokes Equation," *Phys. Rev. Lett.*, (1986) 56, 1505-1508.
2. Genstensen, A.K., Rothman, D.H., "Microscopic modeling of immiscible fluids in three dimensions by a lattice-Boltzmann method," *Europhys. Lett.* (1992) 18, 2, 157-163.
3. Grunau, D., Chen, S., Eggert, K., "A lattice-Boltzmann model for multiphase fluid flows," *Phys. Fluids A*, (1993) 5, 2557-2562.

4. He, X., Doolen, G.D., “Thermodynamic Foundations of Kinetic Theory and Lattice Boltzmann Models for Multiphase Flows,” *Journal of Statistical Physics*, (2002) 107, 1, 309-328.
5. Hou, S., Shan, X., Zou, Q., Doolen, G.D., Soll, W.E., “Evaluation of Two Lattice Boltzmann Models for Multiphase Flows,” *journal of computational physics*, (1997) 138, 695–713.
6. Hou, S., Zou, Q., Chen, S., Doolen, G.D., Cogley, A.C., “Simulation of cavity flow by the lattice Boltzmann method,” *J. Comp. Phys.*, (1995) 118, 329-347.
7. Kang, Q., Zhang, D., Chen, S., “Displacement of a two-dimensional immiscible droplet in a channel,” *Physics of Fluids*, (2002) 14, 3203-3214.
8. Lu, G., Wang, X.D., Duan, Y., “Study on initial stage of capillary rise dynamics,” *Colloids and Surfaces A: Physicochem. Eng. Aspects*, (2013) 433, 95–103.
9. Martys, N. S., Chen, H., “Simulation of multicomponent fluids in complex three-dimensional geometries by the lattice Boltzmann method,” *Phys. Rev. E*, (1996) 53, 743-750.
10. Rothman, D., Zaleski, S., “Lattice-gas models of phase separation: interfaces, phase transitions, and multiphase flow,” *Rev. Modern Phys.*, (1994) 66, 1417-1479.
11. Shan, X., Chen, H., “Lattice Boltzmann model for simulating flows with multiple phases and components,” *Phys. Rev. E*, (1993) 47, 3, 1815-1820.
12. Shan, X., Chen, H., “Simulation of nonideal gases and liquid-gas phase transitions by the lattice Boltzmann equation,” *Phys. Rev. E*, (1994) 49, 4, 2941-2948.
13. Shan, X., Doolen, G.D., “Multicomponent lattice-Boltzmann model with interparticle interaction,” *J. Stat. Phys.*, (1995) 81, 1, 379–393.
14. Swift, M.R., Orlandini, E., Osborn, W.R., Yeomans, J.M., “Lattice Boltzmann simulations of liquid–gas and binary fluid systems,” *Phys. Rev. E*, (1996) 54, 5, 5041–5052.
15. Unsal, E., Mason, G., Morrow, N.R., Ruth, D.W., “Bubble Snap-off and Capillary-Back Pressure during Counter-Current Spontaneous Imbibition into Model Pores,” *Langmuir*, (2009) 25, 3387-3395.
16. Yuana, P., Schaefer, L., “Equations of state in a lattice Boltzmann model,” *physics of fluids*, (2006) 18, 042101.
17. Zou, Q., Hou, S., Chen, S., “An improved incompressible lattice Boltzmann model for time-independent flows,” *J. Stat. Phys.*, (1995) 81, 35–48.